https://doi.org/10.15360/1813-9779-2023-1-2292

3D Spheroids — a Cellular Model for Studying the Effects of Hypoxia on the Epicardial Microenvironment

Konstantin V. Dergilev[1]*, Zoya I. Tsokolaeva[1,2], Irina B. Beloglazova[1], Dmitry O. Traktuev[3], Mohidil T. Rasulova[4], Elena V. Parfenova[1]

[1] Laboratory of Angiogenesis, Experimental Cardiology Institute, Acad. Chazov National Medical Research Center for Cardiology, Ministry of Health of Russia, 15a Cherepkovskaya 3rd Str., 121552 Moscow, Russia
[2] V. A. Negovsky Research Institute of General Reanimatology, Federal Research and Clinical Center of Intensive Care Medicine and Rehabilitology, 25 Petrovka Str., Bldg. 2, 107031 Moscow, Russia
[3] Regenerative Medicine Department, Center for Cardiovascular Medicine, Florida Medical Institute, 1600 SW Archer Rd, M421 Gainesville, FL 32610 USA
[4] Fergana Medical Institute for Public Health, 2A Yangi Turon Str., 150100 Fergana, Fergana region, Uzbekistan

For citation: *Konstantin V. Dergilev, Zoya I. Tsokolaeva, Irina B. Beloglazova, Dmitry O. Traktuev, Mohidil T. Rasulova, Elena V. Parfenova.* 3D Spheroids — a Cellular Model for Studying the Effects of Hypoxia on the Epicardial Microenvironment. *Obshchaya Reanimatologiya = General Reanimatology.* 2023; 19 (1): 43–49. https://doi.org/10.15360/1813-9779-2023-1-2292 [In Russ. and Engl.]

***Correspondence to:** Konstantin V. Dergilev, doctorkote@gmail.com

Summary

Fundamental research in recent years has allowed us to reassess the molecular and cellular mechanisms of cardiac ontogenesis and its repair after damage. The epicardium, the outer, tightly adjoining layer of the cardiac wall formed by epicardial mesothelial cells, collagen and elastic fibers, has gained special relevance as an important participant of reparative processes. Better insight into poorly understood epicardial function is challenged due to anatomical issues and lack of relevant cellular models.

The aim of this study was to develop a spheroid 3D model of the epicardial microenvironment and determine responses of spheroids to hypoxia.

Materials and methods. Spheroids were harvested in V-shaped culture dishes with a low adhesion coating. Immunofluorescent staining of cryosections, histological methods and real-time PCR were used for characterization of cultured spheroids.

Results. We demonstrated that cultivation of cells under low adhesion conditions in V-shaped culture dishes resulted in the formation of spheroids with an average size of 136+21 μm and cell viability rates of over 98%. The cells in the spheroids cultured under normoxic conditions formed tight junctions and were characterized by a low level of proliferation and the ability to synthesize extracellular matrix proteins. Under hypoxia cells in the spheroids showed partial loss of intercellular contacts, acquired a spindle shape, started to express HIF1a, SNAIL, COL1Al and accumulate collagen. All these features demonstrated the activation of mesothelial(endothelial)-mesenchymal transition strongly resembling epicardial cellular responses to ischemia in vivo.

Conclusion. An epicardial spheroid cell culture model suitable for study cellular responses to hypoxic environment was developed. This model can be used to clarify mechanisms regulating epicardial microenvironment and test new targeted candidate drugs.

Keywords: spheroid; hypoxia; cardiac repair

Conflict of interest. The authors declare no conflict of interest.

Read the full-text English version at www.reanimatology.com

Introduction

For several decades, cardiovascular diseases have been the leading cause of morbidity and mortality in Russia and worldwide [1]. The most important factor in the progression of most of these diseases is fibrosis associated with excessive deposition of extracellular matrix proteins, especially fibrillar collagen, leading to increased myocardial stiffness, loss of systolic function, and significant structural and morphological changes [2, 3]. Recently, there has been evidence that the activation of fibrosis can be caused by various factors, which have different effects on the cells and determine the characteristics and rate of the pathological process [4]. The main trigger of fibrosis is hypoxia [5, 6]. It causes stabilization of hypoxia-induced factors (HIF) in cells differentiating into fibroblasts, especially in epicardial cells, provides their activation, fibroblast formation and fibrosis progression [7–9]. However, the mechanisms of such regulation remain poorly understood due to anatomical limitations in accessing the epicardium and the lack of relevant cellular models.

The aim of this study was to develop a 3D model of the epicardial microenvironment and to evaluate the effect of hypoxia on its characteristics.

Material and Methods

Animals.

C57b/6 mice (male, 8 weeks old) were kept in the vivarium of the Yevgeny Chazov National Medical Research Center for Cardiology (Moscow, Russia). The study design was approved by the Ethics Committee of the Institute of Experimental Cardiology.

Simulation of myocardial infarction.

Experimental myocardial infarction in mice was induced according to the previously described protocol [10].

Generation of epicardial mesothelial cell culture.

Epicardial cells were harvested from murine hearts according to the protocol described previously [11].

Assembly of murine epicardial cell spheroids.

For the assembly of epicardial spheroids, we used the GravityTRAPTM ULA Plate (Insphero, USA) V-shaped cups with low adhesion. To obtain spheroids, a cell suspension (5000 cells) was plated into the wells of the plate, precipitated by centrifugation (200 g, 2 min), and cultured for 72 h (in IMDM medium supplemented with 1% fetal calf serum) under standard incubation conditions (37°C, 5% CO_2).

Evaluation of cell viability in spheroids.

The viability of cells forming spheroids was assessed using a commercially available LIVE/DEAD™ Viability/Cytotoxicity Kit (Invitrogen, USA).

Normoxia/hypoxia simulation.

A New Brunswick TM Scientific incubator (Eppendorf, USA) was used to simulate normoxia and hypoxia. Spheroids were cultured under conditions of normoxia and hypoxia (3% O_2) for 72 hours.

Characterization of heart cryosections and spheroids.

To assess the structure of the spheroids, they were stained according to the previously described protocol [12]. Cryosections of spheroids were used for spheroid immunophenotyping experiments. Sections were fixed in 3. 7% para-formaldehyde solution, washed in phosphate-salt buffer solution, preincubated in secondary antibody donor serum solution, and stained with antibodies against the proliferation marker Ki-67 (Abcam, USA), ZO-1 (Abcam, USA), collagen type 1 (Abcam, USA), TCF21 (Abcam, USA), and HIF1a (Abcam, USA) for 1 hour, washed, and stained with antibodies conjugated to Alexa Fluor 488 or 594 (Invitrogen, USA). Cell nuclei were stained with DAPI (Sigma, USA). Morphometric analysis of spheroids was performed using Image J software (NIH, USA).

Preparation of cDNA samples and real-time PCR.

RNA was isolated from cells using a Quiagen kit (Quiagen). Reverse transcription was performed using the Maxima First Strand cDNA Synthesis Kit (Thermo Fisher Scientific). Real-time PCR was performed on a Step One Plus Real-Time PCR System Amplifier (Thermo Fisher Scientific) using a standard protocol with the following primers: SNAIL (ACATCCGAAGCCACACG; GTCAGCAAAAGCACGGTTG), ACTA2 (CCCAGACATCAGGGAGTAATGG; TCTATCGGATACTTCAGCGTCA), FN1 (GGAATGGACCTGCAAACCTA; GTAGGGCTTTCCCAGGTCT), beta actin (CTAAGGCCAACCGTGAAAG; ACCAGAGGCATACAGGGACA), Col1A1 (CCGCTGGTCAAGATGGTC; CTCCAGCCTTTCCTAGGTTCT).

Microscopy and image analysis.

Myocardial cells and cryosections were analyzed using an Axiovert 200 M fluorescence microscope (Carl Zeiss, USA) and AxioVision 4.8 software (Carl Zeiss, USA).

Statistical analysis.

Statistical significance of differences between samples was assessed using the non-parametric Mann–Whitney test. Statistical analysis of the results was performed using Statistica 8.0 software (StatSoft, Inc.). Data were presented as mean±standard deviation (*M*±*SD*).

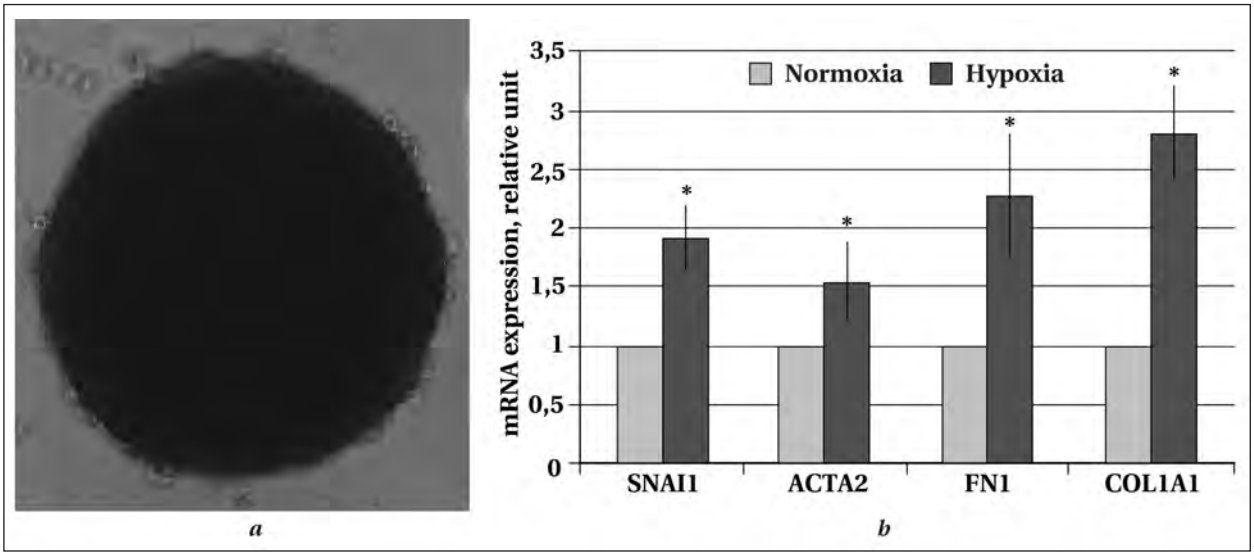

Fig. 1. Characteristics of spheroids created on the basis of epicardial cells.
Note. *a* — Representative image of spheroid created on the basis of murine epicardial cells. *b* — Graphs of quantitative evaluation of SNAI1, ACTA2, FN1, COL1A1 gene expression after spheroid culture under normoxia and hypoxia, * — $P < 0.05$.

Results

Our study showed that culturing cell suspensions under low-adhesion conditions (V-cups with low-adhesion GravityTRAPTM ULA Plate) resulted in accelerated aggregate formation and self-organization of cells into spheroids. We found that cells go through several stages in the process of spheroid assembly: first, a cell cluster is formed, which subsequently compacts to form a globular structure (Fig. 1 *a*). Disappearance of cell processes on the spheroid

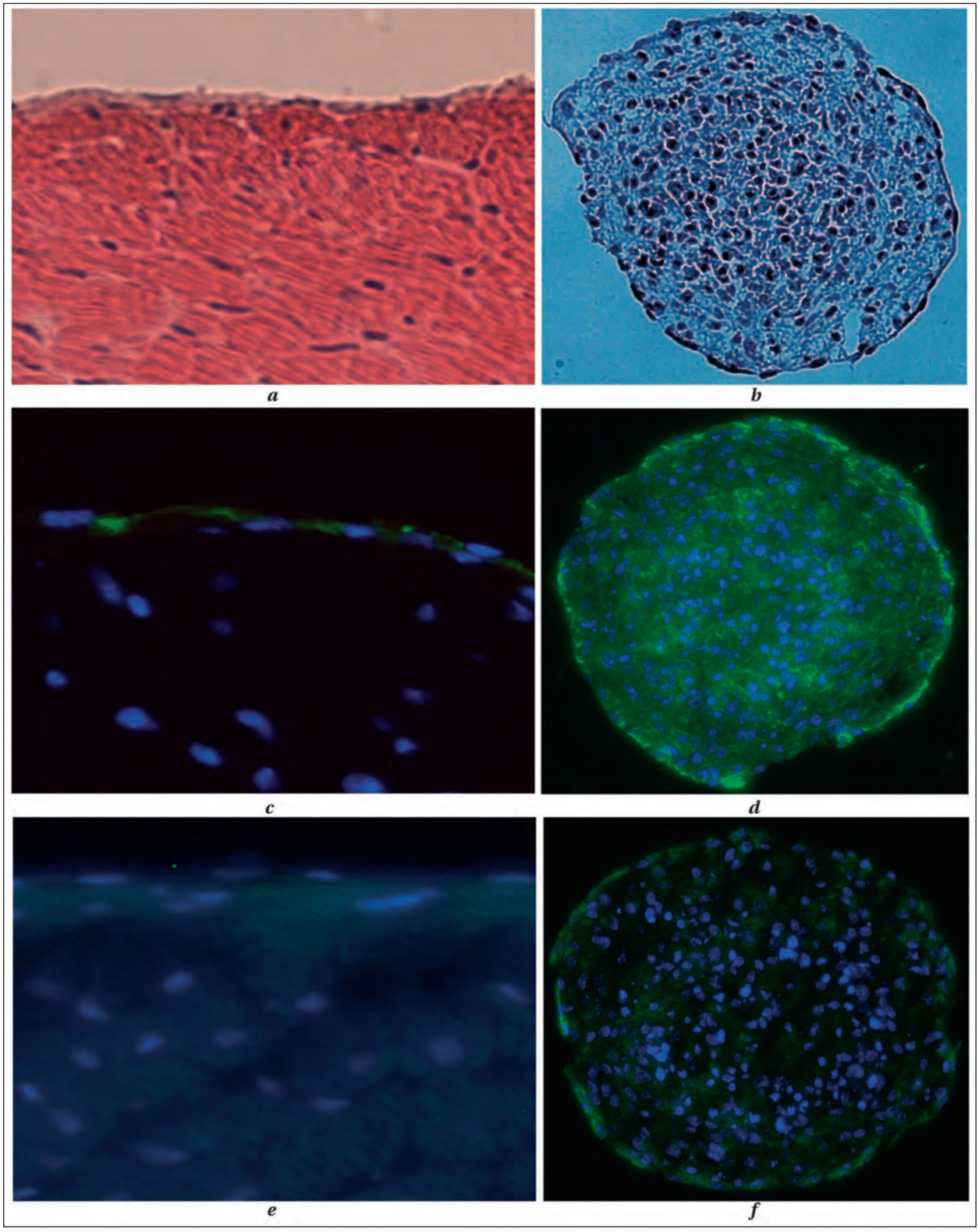

Fig. 2. Comparative characterization of epicardial zone organization in intact heart and spheroid.
Note. Representative images of cryosections of the epicardial zone in the intact heart and spheroid stained with hematoxylin-eosin (*a, b*), antibodies against dense contact protein ZO1 (*c, d, green*), collagen 1 (*e, f, green*). Nuclei were stained with DAPI (*blue*).

surface and formation of a relatively regular spheroid structure occurs 72 hours after plating the cell suspension, indicating the end of spheroid assembly and readiness for subsequent testing. The final size of the formed spheroids was 136+21 μm, and the viability of the cells within them was over 98%.

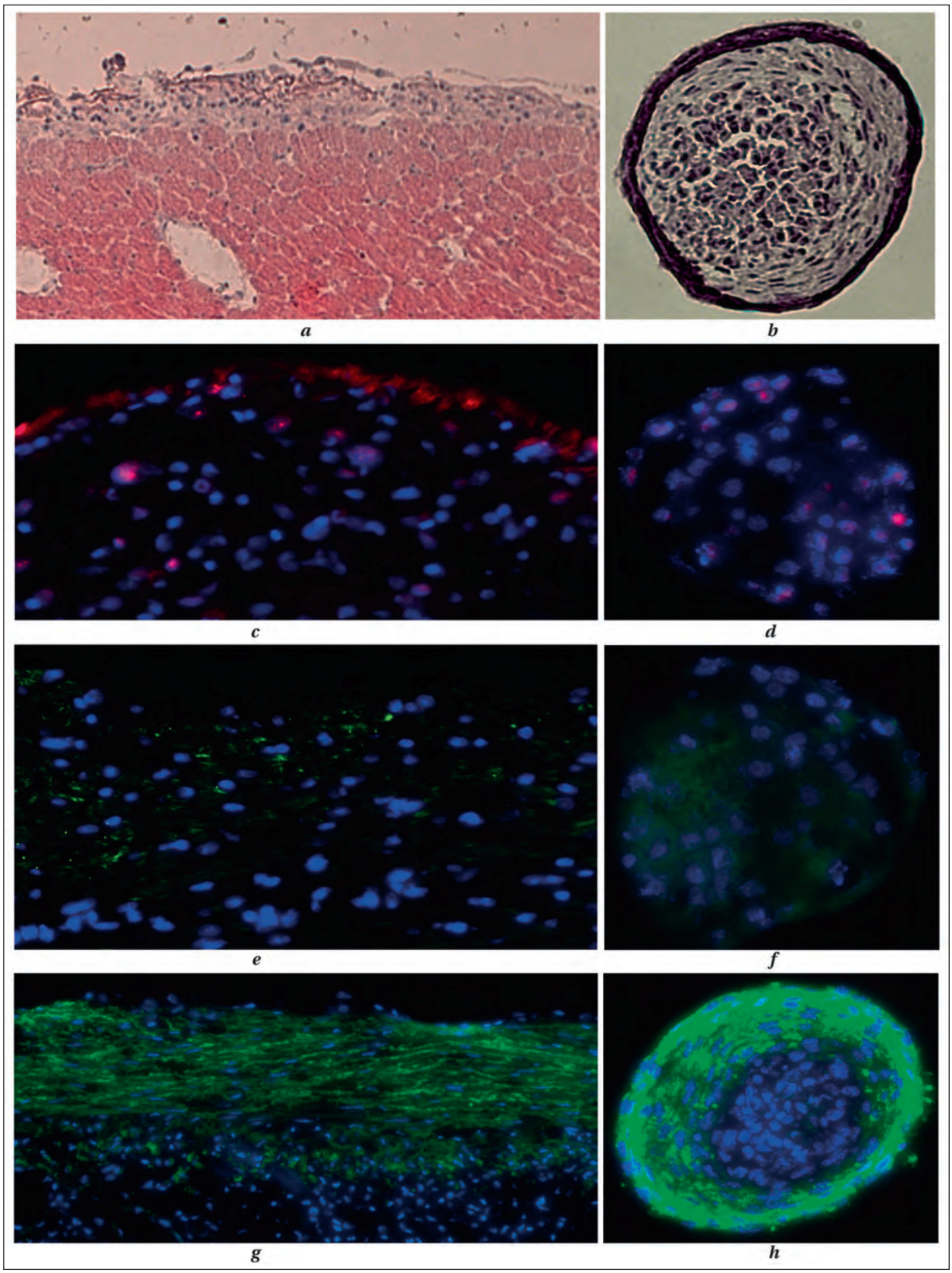

Fig. 3. Comparative characterization of epicardial zone organization in postinfarction heart and in spheroid after hypoxic exposure.
Note. Representative images of cryosections of epicardial zone in intact heart and spheroid stained with hematoxylin-eosin (*a, b*), antibodies against hypoxia marker HIF1a (*c, d, green*), ZO-1 (*e, f, green*), collagen 1 (*g, h, green*). Nuclei were stained with DAPI (*blue*).

The developed model of the epicardial microenvironment should, with a certain degree of assumption, match the pattern of organization of the intact epicardial zone. For this purpose, we compared the structural organization of the epicardial zone in the intact/undamaged heart and in the spheroid (Fig. 2). The spheroid was found to be represented by epicardial cells interacting with each other through ZO-1+ dense contacts, with a low level of expression of fibroblast markers (Fig. 2 *c, d*) and collagen matrix (Fig. 2 *e, f*), which is similar to the organization of the epicardial zone in the intact heart. Simulation of the experimental infarction resulted in an extensive ischemic zone and the appearance of cells expressing HIF1a in the epicardial/subepicardial zone (Fig. 3 *c, d*). After acute ischemic exposure, we observed disorganization of dense contacts between epicardial cells, redistribution, migration of mesothelium into the underlying layers of the cardiac wall, accompanied by thickening of the epicardial area, accumulation of fibroblasts, and increased collagen production (Fig. 3 *e, g*). Similar changes were observed in the generated spheroids cultured under hypoxic conditions. Hypoxic exposure caused loss of intercellular contacts (Fig. 3 *e*), cells acquired a spindle shape (Fig. 3 *b*), expressed HIF1a and accumulated collagen. These changes were accompanied by increased expression of genes associated with activation of the mesothelial-mesenchymal transition (MMT) (SNAI1, ACTA2, FN1, COL1A1) and their differentiation towards fibroblasts/myofibroblasts (Fig. 1 *b*).

Discussion

In the intact heart, epicardial cells are predominantly in a «quiescent» state with low levels of proliferation, no signs of MMT, and a reduced ability to produce extracellular matrix proteins. In contrast, acute ischemic injury has an activating effect on the epicardial cell pool, leading to the initiation of their MMT, increased secretory activity and their migration to the underlying regions of the cardiac wall to participate in repair. Despite the great practical interest in studying the mechanisms of the epicardial regenerative response to damage, its study is difficult due to the lack of relevant models. Currently, the only model described in the scientific literature is based on three-dimensional organotypic epicardial sections of the porcine heart [13], which has significant limitations for its widespread use due to its complex construction, short ex vivo lifespan, and inability to model hypoxic effects. The cell model proposed in this work does not have the above-mentioned drawbacks. The 3D model can be easily generated using commercially available materials/reagents and is able to reproduce, with some assumptions, the changes that occur in the epicardial area under normoxia and hypoxia. Initially, the spheroid is orchestrated by epicardial mesothelial cells interacting through dense ZO-1-containing contacts and exhibiting low levels of expression of fibroblast and collagen matrix markers, which corresponds to the organization of the epicardial zone in the intact heart. Under hypoxia, HIF1a stabilization occurs, epicardial mesothelial cells undergo MMT, acquire fibroblast-like properties and activate the production of extracellular matrix proteins, which correlates with the regenerative response of epicardial cells occurring in the acute phase of cardiac ischemic injury. These findings correlate with those of other researchers who have shown that hypoxia is an important regulator of tissue fibrosis. By acting through the HIF-1 signaling mechanism, hypoxia induces MMT activation, which leads to the loss of E-cadherin-based intercellular contacts, reorganization of the cytoskeleton, and ultimately the production of fibroblast-like cells [14–17]. In contrast, suppression of HIF-1α expression prevented fibroblast formation and reduced ICM accumulation [18]. In addition to its effect on MMT, hypoxia may stimulate fibrogenesis through transcriptional regulation of the expression of genes related to ICM metabolism. Hypoxia induces type I collagen formation, decreases matrix metalloproteinase 2 (MMP-2) levels, and increases the expression of plasminogen activator inhibitor-1 (PAI-1), tissue inhibitor of metalloproteinase-1 (TIMP-1), and connective tissue growth factor (CTGF) through HIF-dependent mechanisms [19–21].

Conclusion

Thus, we have developed and characterized a 3D cellular model of the epicardium capable to exert the cellular responses to hypoxia and be employed in studies of the mechanisms of regulation of the epicardial microenvironment and targeted drugs testing.

References

1. *Mendis S., Graham I., Narula J.* Addressing the global burden of cardiovascular diseases; need for scalable and sustainable frameworks. *Glob Heart*. 2022; 17 (1): 48. DOI: 10.5334/gh.1139. PMID: 36051329.
2. *Raziyeva K., Kim Y., Zharkinbekov Z., Temirkhanova K., Saparov A.* Novel therapies for the treatment of cardiac fibrosis following myocardial infarction. *Biomedicines*. 2022; 10 (9): 2178. DOI: 10.3390/biomedicines10092178.
3. *Scridon A., Balan A.I.* Targeting myocardial fibrosis- a magic pill in cardiovascular medicine? *Pharmaceutics*. 2022; 14 (8): 1599. DOI: 10.3390/pharmaceutics14081599. PMID: 36015225.
4. *Braitsch C.M., Kanisicak O., van Berlo J.H., Molkentin J.D., Yutzey K.E.* Differential expression of embryonic epicardial progenitor markers and localization of cardiac fibrosis in adult ischemic injury and hypertensive heart disease. *J Mol Cell Cardiol*. 2013; 65: 108–119. DOI: 10.1016/j.yjmcc.2013. 10.005. PMID: 24140724.
5. *Wei X., Hou Y., Long M., Jiang L., Du Y.* Molecular mechanisms underlying the role of hypoxia-inducible factor-1 α in metabolic reprogramming in renal fibrosis. *Front Endocrinol (Lausanne)*. 2022; 13: 927329. DOI: 10.3389/fendo.2022.927329. PMID: 35957825.
6. *Steiner C.A., Cartwright I.M., Taylor C.T., Colgan S.P.* Hypoxia-inducible factor as a bridge between healthy barrier function, wound healing, and fibrosis. *Am J Physiol Cell Physiol*. 2022; 323 (3): C866-C878. DOI: 10.1152/ajpcell.00227. 2022. PMID: 35912990.
7. *van den Berg N.W.E., Kawasaki M., Fabrizi B., Nariswari F.A., Verduijn A.C., Neefs J., Wesselink R., Al-Shama R.F.M., van der Wal A.C., de Boer O.J., Aten J., Driessen A.H.G., Jongejan A., de Groot J.R.* Epicardial and endothelial cell activation concurs with extracellular matrix remodeling in atrial fibrillation. *Clin Transl Med*. 2021; 11 (11): e558. DOI: 10.1002/ctm2.558. PMID: 34841686.
8. *Ismail A., Saliba Y., Fares N.* Early development of cardiac fibrosis in young old-father offspring. *Oxid Med Cell Longev*. 2022; 2022: 8770136. DOI: 10.1155/2022/8770136. PMID: 36193084.
9. *Дергилев К.В., Комова А.В., Цоколаева З.И., Белоглазова И.Б., Парфенова Е.В.* Эпикард как новая мишень для регенеративных технологий в кардиологии. *Гены и клетки*. 2020; 14 (2): 33–40. DOI: 10.23868/202004016 [*Dergilev K.V., Komova A.V., Tsokolaeva Z.I., Beloglazova I.B., Parfyonova Ye.V.* Epicardium as a new target for regenerative technologies in cardiology. *Genes & Cells/ Geny i Kletki*. 2020; 14 (2): 33–40. (In Russ.). DOI: 10.23868/ 202004016.
10. *Дергилев К.В., Цоколаева З.И., Белоглазова И.Б., Ратнер Е.И., Молокотина Ю.Д., Парфенова Е.В.* Характеристика ангиогенных свойств c-kit+ клеток миокарда. *Гены и клетки*. 2018; 14 (3): 86–93. DOI: 10.23868/ 201811038. [*Dergilev K.V., Tsokolaeva Z.I., Beloglazova I.B., Ratner E.I., Molokotina Yu.D., Parfyonova Ye.V.* Angiogenic properties of myocardial c-kit+ cells. *Genes & Cells/ Geny i Kletki*. 2018; 14 (3): 86–93. (In Russ.). DOI: 10.23868/ 201811038].
11. *Dergilev K.V., Tsokolaeva Z.I., Beloglazova I.B., Ratner E.I., Parfenova E.V.* Transforming growth factor beta (TGF-β1) induces pro-reparative phenotypic changes in epicardial cells in mice. *Bull Exp Biol Med*. 2021; 170 (4): 565–570. DOI: 10.1007/s10517-021-05107-5. PMID: 33730328.
12. *Massimini M., Romanucci M., De Maria R., Della Salda L.* Histological evaluation of long-term collagen type I culture. *Methods Mol Biol*. 2022; 2514: 95–105. DOI: 10.1007/978-1-0716-2403-6_10. PMID: 35771422.
13. *Maselli D., Matos R.S., Johnson R.D., Chiappini C., Camelliti P., Campagnolo P.* Epicardial slices: an innovative 3D organotypic model to study epicardial cell physiology and activation. *NPJ Regen Med*. 2022; 7 (1): 7. DOI: 10.1038/s41536-021-00202-7. PMID: 35039552.
14. *Kalluri R., Neilson E.G.* Epithelial-mesenchymal transition and its implications for fibrosis. *J Clin Invest*. 2003; 112 (12): 1776–1784. DOI: 10.1172/JCI20530. PMID: 14679171.
15. *Liu Y.* Epithelial to mesenchymal transition in renal fibrogenesis: pathologic significance, molecular mechanism, and therapeutic intervention. *J Am Soc Nephrol*. 2004; 15 (1): 1–12. DOI: 10.1097/01.asn.0000106015.29070.e7. PMID: 14694152.
16. *Iwano M., Neilson E.G.* Mechanisms of tubulointerstitial fibrosis. *Curr Opin Nephrol Hypertens*. 2004; 13 (3): 279–284. DOI: 10.1097/00041552-200405000-00003. PMID: 15073485.
17. *Strutz F., Okada H., Lo C.W., Danoff T., Carone R.L., Tomaszewski J.E., Neilson E.G.* Identification and characterization of a fibroblast marker: FSP1. *J Cell Biol*. 1995; 130 (2): 393–405. DOI: 10.1083/jcb.130.2.393. PMID: 7615639.
18. *Higgins D.F., Kimura K., Bernhardt W.M., Shrimanker n., Akai Y., HohensteinB., Saito Y., Johnson R.S., Kretzler M., Cohen C.D., Eckardt K-U., Iwano M., Haase V.H.* Hypoxia promotes fibrogenesis in vivo via HIF-1 stimulation of epithelial-to-mesenchymal transition. *J Clin Invest*. 2007; 117 (12): 3810–3820. DOI: 10.1172/JCI30487. PMID: 18037992.
19. *Orphanides C., Fine L.G., Norman J.T.* Hypoxia stimulates proximal tubular cell matrix production via a TGF-beta1-independent mechanism. *Kidney Int*. 1997; 52 (3): 637–647. DOI: 10.1038/ki.1997.377. PMID: 9291182.

20. *Kietzmann T., Roth U., Jungermann K.* Induction of the plasminogen activator inhibitor-1 gene expression by mild hypoxia via a hypoxia response element binding the hypoxia-inducible factor-1 in rat hepatocytes. *Blood*. 1999; 94 (12): 4177–4185. DOI: 10.1182/blood.V94.12.4177.

21. *Higgins D.F., Biju M.P., Akai Y. Wutz A., Johnson R.S., Haase V.H.* Hypoxic induction of Ctgf is directly mediated by Hif-1. *Am J Physiol Renal Physiol*. 2004; 287 (6): F1223–F1232. DOI: 10.1152/ajprenal.00245.2004. PMID: 15315937.

Received 25.11.2022
Accepted 20.12.2022